Molecular analyses provide insight into mechanisms underlying sarcopenia and myofibre denervation in old skeletal muscles of mice

Mitchell Barns [a], Cedric Gondro [b], Ross L. Tellam [c], Hannah G. Radley-Crabb [a,d], Miranda D. Grounds [a], Tea Shavlakadze [a,*]

[a] *School of Anatomy, Physiology and Human Biology, the University of Western Australia, WA, Australia*
[b] *The Centre for Genetic Analysis and Applications, University of New England, Armidale, New South Wales, Australia*
[c] *CSIRO Animal, Food and Health Sciences, Queensland Biosciences Precinct, Queensland, Australia*
[d] *School of Biomedical Sciences, Faculty of Health Sciences, Curtin University, Western Australia, Australia*

ARTICLE INFO

ABSTRACT

Molecular mechanisms that are associated with age-related denervation and loss of skeletal muscle mass and function (sarcopenia) are described for female C57Bl/6J mice aged 3, 15, 24, 27 and 29 months (m). Changes in mRNAs and proteins associated with myofibre denervation and protein metabolism in ageing muscles are reported, across the transition from healthy adult myofibres to sarcopenia that occurs between 15 and 24 m. This onset of sarcopenia at 24 m, corresponded with increased expression of genes associated with neuromuscular junction denervation including *Chnrg*, *Chrnd*, *Ncam1*, *Runx1*, *Gadd45a* and *Myog*. Sarcopenia in quadriceps muscles also coincided with increased protein levels for Igf1 receptor, Akt and ribosomal protein S6 (Rps6) with increased phosphorylation of Rps6 (Ser235/236) and elevated Murf1 mRNA and protein, but not Fbxo32: many of these changes are also linked to denervation. Global transcription profiling via microarray analysis confirmed these functional themes and highlighted additional themes that may be a consequence of pathology associated with sarcopenia, including changes in fatty acid metabolism, extracellular matrix structure and protein catabolism. Ageing was also associated with increased global gene expression variance, consistent with decreased control of gene regulation.

© 2014 Elsevier Ltd. All rights reserved.

1. Introduction

The age-related loss of skeletal muscle mass and function, called sarcopenia, adversely affects movement, mobility, posture, metabolism, independence and mortality. The incidence of sarcopenia is reported as 14% by 65–69 years of age, may reach greater than 50% by 80 years (Janssen, 2010) and loss of function may occur before loss of muscle mass (Clark and Manini, 2008). Sarcopenia results in diminished independence and frailty that increases the risk of falls and fractures with escalating costs for the global health system (Cruz-Jentoft, 2010). As the human population rapidly ages, there is a compelling need to better understand the molecular mechanisms that cause sarcopenia in order to design and implement the best early intervention strategies.

The extent of sarcopenia is highly variable and depends on factors such as ethnicity, diet, health status, gender, activity, lifestyle and muscle type (Janssen, 2010). The precise reasons for sarcopenia are not well understood, however the general age related decrease in hormonal and nervous system capacity are proposed as contributors (Sayer et al., 2013; Shavlakadze and Grounds, 2003), with interactions between many systemic and local factors at the tissue level (McMahon et al., 2010). At the myofibre level, a wide range of mitochondrial and metabolic changes have been described (Altun et al., 2010; Calvani et al., 2013; Rennie et al., 2010). We have a particular interest in the innervation of myofibres, since electrical stimulation by a nerve is essential for normal muscle function and maintenance of muscle mass (Faulkner et al., 2007).

Denervation of myofibres has been demonstrated in old mice (Chai et al., 2011; Valdez et al., 2010; Yang et al., 2011) and elderly humans (Aagaard et al., 2010) where it is more pronounced, probably due to the longer ageing time of more than 30 years for humans (from ~60 to >90 years of age) compared with only about 1.5 years for rodents. The mouse is especially useful as a model of sarcopenia due to the many genetically modified mouse lines that can help elucidate specific mechanisms in the future. For species comparison,

3, 15 and 24 m old mice are roughly equivalent to humans aged 20, 50 and 70 years (Flurkey et al., 2007).

We have previously described the time-course of sarcopenia development in female C57Bl/6J mice, with significant loss of quadriceps muscle mass by 24 m that is more pronounced by 27–29 m (Shavlakadze et al., 2010b), at a time where there is denervation and altered NMJ morphology of myofibres (Chai et al., 2011). The present study used tissues from these same mice to investigate the mechanisms that lead to this loss of muscle mass: specifically the expression of genes and proteins that coincide with, or potentially precede, muscle loss and myofibre denervation were analyzed, with the aim to identify biomarkers to monitor the onset and progression of sarcopenia.

Denervation results in myofibre atrophy with a net loss of muscle protein, through complex interacting signalling pathways that regulate the balance between protein synthesis and degradation. Since signalling downstream from the Insulin-like growth factor-1 (IGF-1) and insulin receptors is of central importance for regulation of protein metabolism and maintenance of normal muscle mass (Schiaffino and Mammucari, 2011; Shavlakadze and Grounds, 2006), activities of key proteins in this pathway were also measured in ageing skeletal muscles in the present study. The power of our study is the comprehensive analysis of many molecular changes (using qRT-PCR, immunoblotting and microarrays) at five ages (from 3 to 29 m), to define the progression of events that result in sarcopenia, especially during the transition between healthy adults and the onset of sarcopenia (15–24 m), in mice.

2. Materials and methods

2.1. Mice and tissue collection

Female C57Bl/6J mice aged 15, 24, 27 and 29 m were obtained from an ageing colony at Royal Brisbane Hospital, Queensland. Female C57Bl/6J mice aged 3 m were obtained from the Animal Resource Centre, Murdoch, Western Australia. All mice were maintained on a 12 h light: 12 h dark regimen at 22 °C, with free access to mouse and rat diet (Specialty Feeds, Australia) and water. Mice were delivered to the University of Western Australia (UWA) and allowed to acclimate for one week. All animal procedures were carried out in accordance with the National Health and Medical Research Council of Australia and approval by the UWA Animal Ethics Committee. Mice were anaesthetized with a gaseous mixture of 2% isoflurane 400 cc/min NO_2 and 1500 cc/min O_2 and killed by cervical dislocation. Gastrocnemius and quadriceps were removed and snap frozen in liquid nitrogen for mRNA and protein analyses. Quadriceps muscles were embedded for cryo-sectioning as described in (Shavlakadze et al., 2010a).

2.1.1. Histology and immunohistochemistry

Quadriceps cryo-sections were stained with haematoxilin and eosin (H&E) or immuno-stained with Desmin antibody, 1:300 dilution (abcam, ab8592). Myofibres with non-peripheral nuclei were quantified only in the rectus femoris part of the quadriceps using 4 individual images taken at $10\times$ magnification from each muscle.

2.1.2. Quadriceps RNA extraction and qRT-PCR

Quadriceps muscles ($n = 4$–6 per group) were ground in liquid nitrogen and the resulting powder split into two portions for RNA and protein extraction. Procedures for RNA extraction and cDNA preparation have been described elsewhere (Shavlakadze et al., 2013b). Primers purchased from Qiagen are listed in Supplementary Table S1. Gene expression in skeletal muscle was normalized to the geometric mean of *Hprt1* and *Ppia* expression values using the GeNorm algorithm (Vandesompele et al., 2002). The mRNA

levels for these genes were similar at all five ages (Supplementary Fig. S1A and B).

2.1.3. Protein extraction and immunoblotting

Protein fractions (soluble and insoluble in 1% NP40) were extracted from quadriceps muscles. Muscle powder was homogenized with a Polytron homogenizer in $\times5$ (v/w) ice-cold PBS, 1% NP40, 1 mM EDTA, supplemented with complete EDTA-free protease and phosphatase inhibitor tablets (Roche, Mannheim, Germany) and centrifuged ($13,000 \times g$, 20 min). The supernatant represents the 1% NP40 soluble protein fraction. The resultant pellets were solubilized by sonication in a buffer containing 20 mM HEPES and 4% SDS supplemented with protease and phosphatase inhibitor tablets (Roche, Mannheim, Germany), followed by centrifugation ($19,600 \times g$, 10 min) (Shavlakadze et al., 2013a). Protein was quantified with the DC^{TM} protein assay (Bio-Rad) and samples were resolved on 4–15% SDS-PAGE TGX gels (Bio-Rad, NSW, Australia) and transferred onto nitrocellulose membrane using a Trans Turbo Blot system (Bio-Rad, NSW, Australia). Immunoblotting was performed with antibodies to p-Akt(Ser473) (#9271), t-Akt (#9272), p-ribosomal protein S6(Ser235/236) (#4858), and t-ribosomal protein S6 (#2217), all from Cell Signaling (all 1:1000 in 5% BSA) and antibodies to Murf1/Trim3 (0.1 μg/ml in 5% BSA) (AF5366, R&D systems) and Fbxo32 (1:1000 in 5% BSA) (SAB2501208, Sigma Chemical Co., St Louis, MO, USA). The 'p' and 't' prefixes signify 'phosphorylation' and 'total', respectively. HRP-conjugated secondary antibodies were from Thermo Fisher Scientific, MA, USA. Chemiluminescence signal was captured with ChemiDoc MP Imaging System (Bio-Rad). Resultant images were quantified using ImageJ software. A common sample was loaded on each gel to normalize for detection efficiencies across membranes. All immunoblot images in the figures represent samples immunoblotted onto the same membrane.

2.1.4. Statistical analyses

Gene expression data obtained by qRT-PCR and protein expression data obtained by immunoblotting were analyzed using one-way ANOVA followed by Fisher's Least Significant Difference (LSD) as the Post Hoc test for statistical analysis for direct comparisons between individual means. The significance threshold was set at $P \leq 0.05$. Data are shown as mean ± standard error of mean.

2.2. Variance analysis of microarray and qRT-PCR data

The $\log_2$ RMA normalized microarray data were filtered to remove control probes and probes with low average expression intensities (<8). Variances for each probe were calculated across the dataset and within each age group and a simple median centered Levene test was used to test for differences in variances between the age groups. Variance ratios (σ_g^2/σ_t^2) per age group for each probe were then calculated and pairwise F-ratios estimated. The same approach was used for the qRT-PCR gene expression data.

2.3. Gastronemius RNA extraction for microarray analyses

Total RNA was extracted from gastrocnemius muscles using Trizol reagent (Invitrogen). Samples from four animals were extracted at each of the four ages, i.e. 3, 15, 24 and 29 m. The RNA was quantified spectrophotometrically and its integrity validated by the OD_{260}/OD_{280} absorption ratio (>1.8) and by visualization on an agarose gel. The quality of RNA was assessed by Agilent 2100 Bioanalyzer, RNA 6000 Nano LabChip kit and Agilent 2100 Expert Software (Agilent Technologies, Inc., Santa Clara, CA, USA). All samples with RIN scores >7.5 were selected for the microarray experiment.

2.4. Microarray transcript profiling

The murine MGGE_AGHS1C_8 × 60 K Agilent SurePrint G3 GE microarray was employed for transcriptional analyses of the samples by Agilent services. The microarray contains 39,430 Entrez genes and 16,251 lncRNA (murine RefSeq build 37). The target labeling was performed using Cy3 and the Agilent Amplification Kit PLUS (Agilent, #5184-3523) according to the manufacturer's instructions. The microarray slides were washed, scanned using an Agilent microarray scanner (G2505B) and signal intensities extracted using Agilent feature extraction software.

The target labelling, hybridisations, fluidics and chip scanning were performed according to the manufacturer's instructions. Quality control measures, pre-processing and analyses were performed using the statistical computing language R and Bioconductor (Gentleman et al., 2004). All microarray images and quality control measurements were within recommended limits. The quality of the arrays was assessed through standard measures: pseudo-images of the arrays (detects spatial effects), scatter plots of the arrays versus a pseudo-median reference chip, and other summary statistics including histograms and box-plots of raw log intensities, signal-to-noise ratios, box-plots of normalized log ratios. Transcription intensities ($\log_2$ scale) were estimated after normalization using RMA (Irizarry et al., 2003a, 2003b). Briefly, the background was corrected by convolution and the data were then quantile normalized and summarized by median polish. Prior to testing for differential expression, the data were filtered to remove control spots and spots with no signal in over 50% of the slides. Duplicated probes were pooled into a single average intensity read, thus leaving around 15,000 features to be tested in each age contrast.

Differential expression between each pair of adjacent ages was tested on a gene by gene basis using a moderated *t*-test with intensities adjusted using an Empirical Bayes approach (Smyth, 2004). This approach was used to focus the analysis on the progressive changes in gene expression compared with the immediately earlier age. A covariance structure to account for within array variability was also fitted in the model. Features were considered significantly differentially expressed for a false discovery rate adjusted *P*-value of 0.01, using the Benjamini–Hochberg correction. A minimum fold change of 2 was used as an additional filter. Thus, the analysis of the microarray data used a conservative approach. Data were deposited in NCBI's Gene Expression Omnibus (GSE53959). Supplementary File S1 is an HTML report containing all pre-processing analyses, annotated lists of differentially expressed genes between adjacent ages with gene intensity level ($\log_2$ scale) and *P*-value, links to NCBI, Gene Ontology and KEGG pathway analyses and quality control images. Fold changes were defined as the older age relative to the younger age in each age contrast.

2.5. Functional enrichment analyses

Functional enrichment profiles for the differentially expressed genes in each age contrast were derived for each of the Gene Ontology (GO) categories: Cellular Component, Molecular Function and Biological Process, as well as enriched KEGG pathways (Supplementary File S1). The gene function analyses used conservative approaches. Differentially expressed genes were mapped from their Entrez identifier to their most specific GO term and these were used to span the tree structure and test for enriched function terms. Profiles for each category were also constructed for the differentially expressed genes for different tree depths. To avoid over-inflated *P*-values, the background consisted exclusively of the array probes used in the analyses after the removal of control probes, non-expressed probes and un-annotated probes. Statistical significance of the functional term enrichment was determined
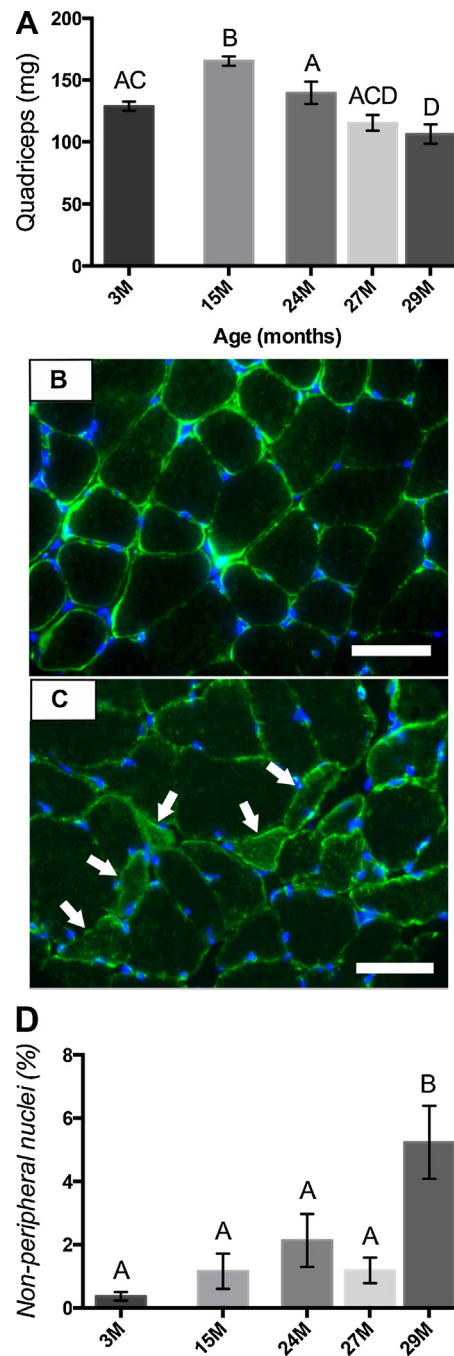

Fig. 1. Quadriceps femoris muscle weights in female C57Bl/6J mice aged 3 to 29 months (m) (A), quadriceps muscle cross sections from 3 and 24 m old mice immunostained with desmin (B and C) and proportion of myofibres with non-peripheral myonuclei in quadriceps (D). Muscle weight data (A) are mean ± s.e.m for 6–11 mice/group and means without a common letter are significantly different at $P \leq 0.05$, ANOVA with Fisher's LSD tests. Desmin immunostaining (B and C) depicts myofibres with uniform appearance at 3 m (B) and atrophic, misshaped myofibres at 24 m (C and arrows). Scale bar, 50 μm. The proportion (%) of myofibres with non-peripheral myonuclei/total number of myofibres (D) was quantified in cross-sections of the *rectus femoris* part of the quadriceps stained with H&E. *Note*: In all histograms (Figs. 1–6 and Supplementary Fig. S1) a decreasing interval between bars (on the *X*-axis) indicates a decreasing age gap between the older groups.

using a weighted scoring algorithm implemented in the topGO R package (Alexa and Rahnenfuhrer, 2013). For completeness, three additional methods (Fisher, Kolmogorov–Smirnov and elimination) were also included in Supplementary File S1 but are not discussed in the manuscript as they provided overlapping information. Enriched
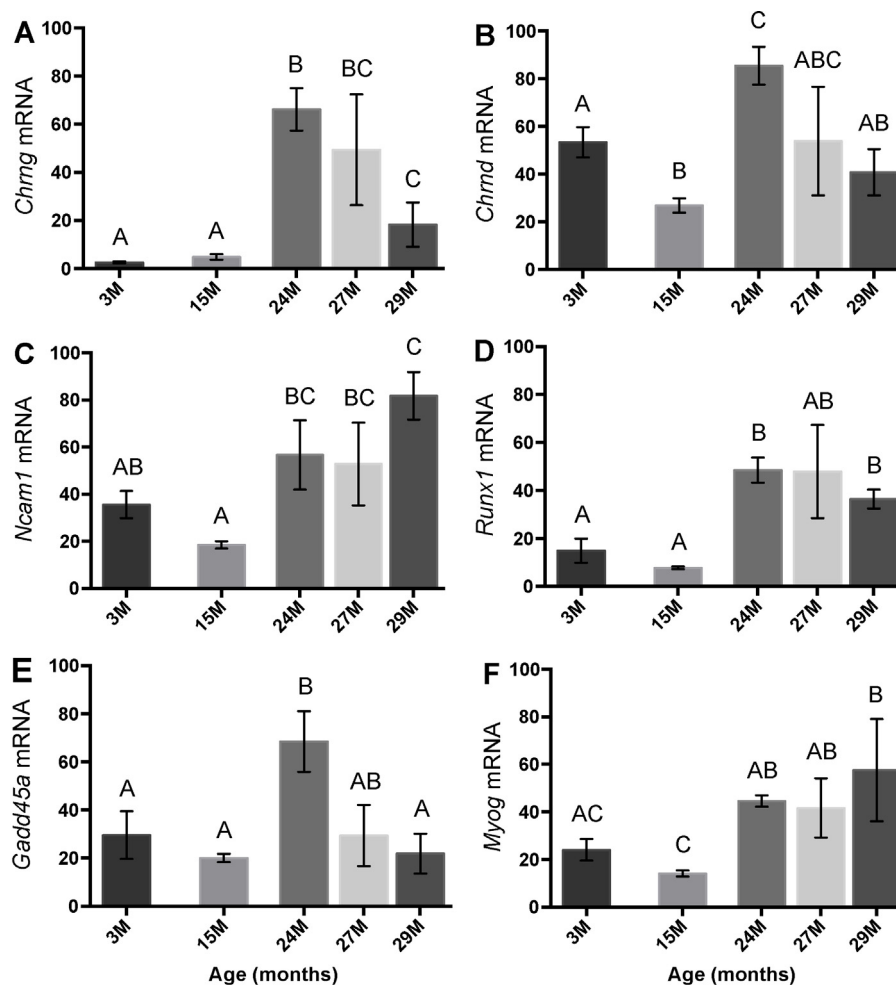
Fig. 2. *Chrng* (A), *Chrnd* (B), *Ncam1* (C), *Runx1* (D), *Gadd45a* (E) and *Myog* (F) mRNA in quadriceps muscles aged 3 to 29 m. Data are mean ± s.e.m. from 4 to 6 mice per group. Means without a common letter are significantly different at $P \leq 0.05$, ANOVA with Fisher's LSD tests. *Y*-axis represents arbitrary units.

GO terms include those with a significance value of $P < 0.01$. KEGG pathway enrichment was measured in a similar manner but with a hypergeometric test to compute *P*-values.

To identify higher level functional themes, the Database For Annotation, Visualization And Integrated Discovery (DAVID) with a background containing all murine annotated genes present on the microarray was used (Huang da et al., 2009). Differentially expressed genes were independently analyzed according to their direction of change in each age contrast. DAVID groups annotations into clusters based on overlaps of genes associated with each function term. This generates a Functional Annotation Cluster that gives a clearer overview of enriched gene function information associated with large datasets. Default parameters were used in the analysis. The geometric mean of the *P*-values for the terms in each Functional Annotation Cluster was calculated. Values less than or equal to 0.1 were considered significant. The enrichment score for each cluster was defined as the LOD score. Functional Annotation Clusters were then manually grouped into Functional Themes.

3. Results

3.1. Quadriceps muscle weights and morphology

We have extensively described the age related morphological changes in limb muscles of female C57Bl/6J mice used in this study (Chai et al., 2011; Shavlakadze et al., 2010b; Tohma et al., 2011). In brief, the quadriceps muscle mass was lower at 24 m compared with 15 m and further decreased by 27 and 29 m, demonstrating progressive loss of muscle mass with ageing (Shavlakadze et al., 2010b) (Fig. 1A). Mis-shaped, flattened atrophic myofibres with peripheral myonuclei were observed in quadriceps from mice aged ≥24 m (Fig. 1C): these were not present in young muscles (Fig. 1B). Myofibres with non-peripheral (central or displaced) myonuclei were counted in quadriceps muscle cross-sections (Fig. 1D) as these may indicate regenerated myofibres. Number of myofibres with displaced nuclei increased in very old (29 m) muscles, however this number was relatively low (~5% of the total myofibre number). In our study, in old female C57Bl/6J quadriceps, there was no conspicuous indication that necrosis or regeneration was occurring, since areas of fragmented sarcoplasm with inflammation and young myotubes were not observed histologically. Thus, myofibres with displaced nuclei may reflect very low levels of necrosis/regeneration, or denervation may be responsible for the internalization of nuclei.

3.2. Expression of genes regulated by innervation in ageing quadriceps muscles

To substantiate our cellular observations of increased numbers of denervated NMJs in old extensor digitorum longus (EDL) muscles of C57Bl/6J female mice (Chai et al., 2011), we performed qRT-PCR quantification of nicotinic acetylcholine receptor (nAChR) gamma and delta subunits (*Chrng* and *Chrnd*), neural cell adhesion molecule 1 (*Ncam1*), runt-related transcription factor-1 (*Runx1*),

growth arrest and DNA damage-inducible 45α (*Gadd45α*) and Myogenin (*Myog*) in quadriceps (Fig. 2A–F), because expression of these genes increases in denervated muscles (Adams et al., 1995; Bongers et al., 2013; Dedkov et al., 2003; Kostrominova et al., 2000; Wang et al., 2005; Zhu et al., 1994).

Loss of innervation is associated with the expression of all nAChR subunits and promotes re-expression of the embryonic γ subunit (Adams et al., 1995; Hall and Sanes, 1993). In line with this evidence, there was a striking (∼12-fold) increase in *Chrng* mRNA expression at 24 m compared with 15 m ($P \leq 0.005$) (Fig. 2A). The amount of *Chrng* mRNA decreased from 24 to 29 m ($P \leq 0.05$), but was still higher in old groups compared with young (3 and 15 m) (Fig. 2A). *Chrnd* mRNA also increased (2.2-fold higher) from 15 to 24 m ($P \leq 0.05$) and decreased thereafter in older muscles (Fig. 2B). *Ncam1* mRNA levels were higher in all old groups compared with 15 m ($P \leq 0.05$) (Fig. 2C).

Up-regulation of *Runx1* in denervated muscle has a protective role from severe muscle atrophy (Wang et al., 2005). In our study, *Runx1* mRNA increased substantially from 15 to 24 m ($P \leq 0.005$) and remained high in all old groups compared with young (3 and 15 m) (Fig. 2D). *Gadd45a*, which promotes denervation induced myofibre atrophy (Bongers et al., 2013) was also induced in ageing quadriceps muscles between 15 and 24 m (Fig. 2E).

We next measured expression of the myogenic regulatory factors, Myogenin (*Myog*) and MyoD1 (*Myod1*) in ageing quadriceps, since expression of both genes increases in surgically denervated muscles (Dedkov et al., 2003; Eftimie et al., 1991; Kostrominova et al., 2000; Moresi et al., 2010). *Myog* mRNA increased from 15 m to 24 m ($P \leq 0.05$) and remained elevated from 24 to 29 m (Fig. 2F). *Myod1* mRNA increased only in very old (29 m) muscles, albeit with high individual variation within the group ($P \leq 0.05$) (Supplementary Fig. S1C).

Thus, significantly increased expression of *Chrng*, *Chrnd*, *Ncam1*, *Runx1*, *Gadd45a* and *Myog* in ageing quadriceps muscles coincides with the transition to sarcopenia, from 15 to 24 m, in the female C57Bl/6J mice.

3.3. Factors involved in protein homeostasis

We analyzed mRNA and protein expression for the IGF-1 receptor (Igf1r) β-subunit, expression and phosphorylation of Akt and Rps6 that constitute the anabolic signalling pathway, and expression of two E3-ubiquitin ligases, muscle RING finger protein-1 (Murf1) and muscle atrophy F-box protein 32 (Fbxo32), involved in the proteasomal protein degradation pathway (Glass, 2003; Schiaffino and Mammucari, 2011).

3.3.1. IGF-1 receptor

Igfr1 mRNA decreased at 24 m compared with 15 m ($P \leq 0.005$), however muscles of older (27 and 29 m) mice had similar levels to 3 and 15 m old mice (Fig. 3A). Igf1r protein levels did not reflect changes in the mRNA and were higher at all old ages (24, 27, 29 m) compared with 15 m ($P \leq 0.05$) (Fig. 3B and C).

3.3.2. Akt and RpS6

We measured mRNAs for two Akt genes, *Akt1* and *Akt2* (Nader, 2005) in quadriceps and found that *Akt1* mRNA levels were similar at 3–27 m, but increased at 29 m ($P \leq 0.05$) (Fig. 4A). In contrast, *Akt2* mRNA decreased from 3 to 15 m ($P \leq 0.05$) and, although there was a trend for increased *Akt2* expression in older muscles, the levels were not significantly different between 15 and 29 m (Fig. 4B). We next measured protein levels for total (t-Akt) and phosphorylated Akt (p-Akt) in ageing quadriceps muscles (Fig. 4C–E). Amounts of p-Akt (Ser473) relative to t-Akt (antibody detects both total Akt1 and Akt2), which reflect activation of this protein, were similar at all ages (Fig. 4C and D). T-Akt protein (standardized to Ponceau S
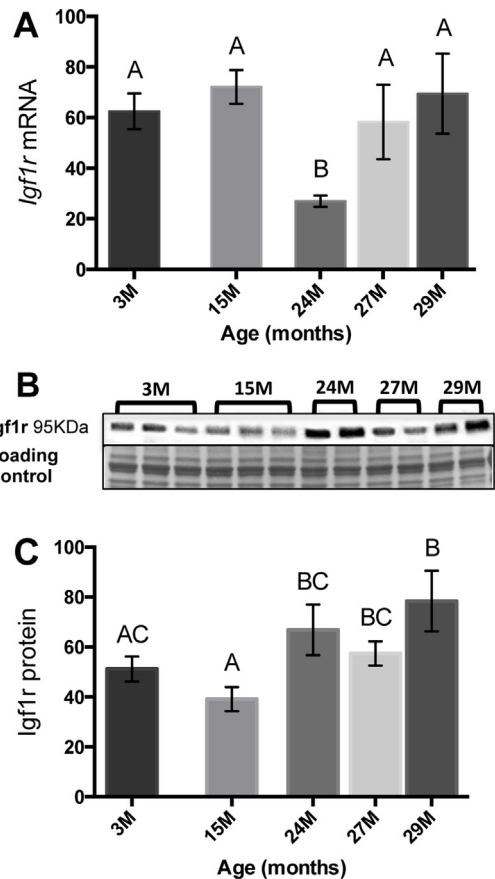

Fig. 3. *Igf1r* mRNA (A) and protein (B and C) in quadriceps muscles aged 3–29 m. *Igf1r* mRNA (β-subunit) was quantified in 4–6 mice per group (A). For immunoblots, equal loading was confirmed by staining membranes with Ponceau S (B). Igf1r protein (β-subunit) (C) was quantified relative to a Ponceau S stained band from the same membrane located at ∼23 kDa (B). Protein quantification is based on 4 mice/group. All data (A and C) are mean ± s.e.m and means without a common letter differ, $P \leq 0.05$, ANOVA with Fisher's LSD tests. Y-axis represents arbitrary units.

stained band located at ∼23 kDa, Fig. 4C) decreased from 3 to 15 m ($P \leq 0.05$) and increased from 15 to 24 m to levels similar to 3 m ($P \leq 0.05$), remaining unchanged at later ages (Fig. 4C and E).

Rps6 mRNA levels were similar at all ages, except for 24 m, where expression decreased ($P \leq 0.005$) compared with 15 m (Fig. 5A). Amounts of phosphorylated Rps6 (p-Rps6(Ser235/236)) relative to total Rps6 (t-Rps6) were substantially lower at 15 m compared with 3 m ($P \leq 0.05$) (Fig. 5B and C), however in muscles aged ≥24 m, p-Rps6(Ser235/236) levels increased relative to 15 m and were similar to those in 3 m old muscles (Fig. 5B and C). T-Rps6 protein levels standardized to a ∼23 kDa Ponceau S stained band were similar at all ages except for 15 m, where t-Rps6 was lower compared with younger and older muscles ($P \leq 0.005$) (Fig. 5B and D). This result contrasts with the age-related changes in Rps6 mRNA expression (Fig. 5A).

3.3.3. Murf1 and Fbxo32

We quantified mRNA and protein for Murf1 and Fbxo32 in quadriceps muscles at the five ages. *Murf1* mRNA levels were 1.3- and 1.6-fold higher at 24 and 29 m respectively, compared with 15 m ($P \leq 0.05$) (Fig. 6A). Expression levels were similar at 3, 15 and 27 m, but low relative to 24 and 29 m ($P \leq 0.05$) (Fig. 6A). Murf1 protein was quantified in the 1% NP40 insoluble fraction enriched with contractile proteins (Clarke et al., 2007; Shavlakadze et al., 2013b), because Murf1 facilitates degradation of myosins (Clarke et al., 2007; Cohen et al., 2009). The increase in *Murf1* mRNA
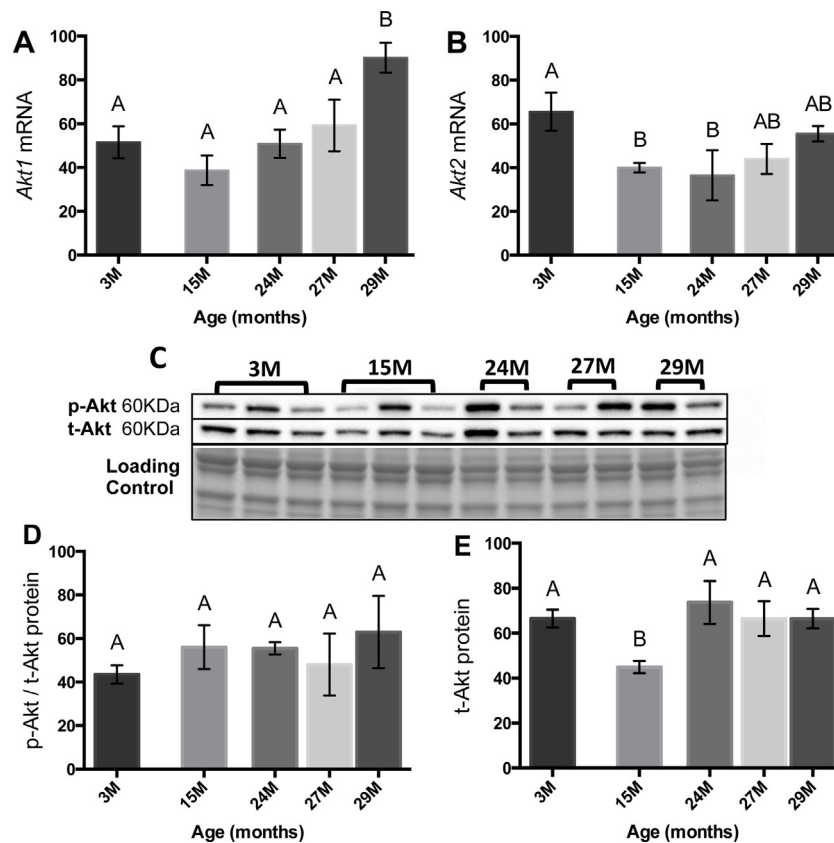
Fig. 4. Akt mRNA and protein in quadriceps muscles aged 3–29 m. *Akt1* (A) and *Akt2* (B) mRNA was quantified in 4–6 mice per group. For immunoblots, equal loading was confirmed by staining membranes with Ponceau S (C). p-Akt(Ser473) was quantified relative to t-Akt (D) and t-Akt (E) was quantified relative to a Ponceau S stained band from the same membrane located at ∼23 kDa (C). Protein quantification is based on 4 mice/group. Data (A, B, D and E) are mean ± s.e.m and means without a common letter differ, $P \leq 0.05$, ANOVA with Fisher's LSD tests. *Y*-axis represents arbitrary units.

from 15 to 24 m was reflected by a similar increase in Murf1 protein associated with the 1% NP40 insoluble fraction ($P \leq 0.0001$) (Fig. 6B and C). Murf1 protein levels were similar at all other ages.

Fbxo32 mRNA expression also displayed age-related changes, and was higher at 15 m compared with all other ages ($P \leq 0.005$) (Fig. 6D). Fbxo32 protein amounts were less affected by age, although a decrease was seen between 27 and 29 m ($P \leq 0.05$) (Fig. 6E and F).

3.4. Microarray transcriptional profiling of ageing skeletal muscles

Microarrays were used to investigate age-related changes in gene expression in gastrocnemius muscles from the same female C57Bl/6J mice aged 3–29 months. This approach complements the targeted gene expression analyses for quadriceps muscles, and has the potential to identify additional functional themes associated with the onset and progression of sarcopenia. Supplementary File S1 (http://www.ncbi.nlm.nih.gov/geo/query/acc.cgi?acc=GSE53959) lists details of the differentially expressed genes for each adjacent age contrast, as well as enriched Gene Ontology (GO) Molecular Function (MF), Cellular Content (CC) and Biological Process (BP) categories for each of the 3 age contrasts (15 vs 3 m; 24 vs 15 m, and 29 vs 24 m). Also included are enriched KEGG pathways.

A much larger number of genes (835) was differentially expressed between 29 and 24 months compared with the two earlier age contrasts (375 and 170 genes, respectively) (Supplementary Table S2). The transcriptional changes occurring between 29 and 24 m also corresponded with the period of greatest loss of muscle mass, suggesting that transcriptional deregulation was associated with the physiological consequences of sarcopenia and/or general ageing.

To obtain a high level perspective of the gene expression changes, the DAVID functional analysis tool (Huang da et al., 2009) was used to group significantly enriched terms into *Functional Annotation Clusters*. Clusters with enrichment scores (- $\log_{10}$ mean of cluster term *P*-values) greater than 1.0 were considered significant. The full analysis is available in Supplementary Table S3. *Functional Annotation Clusters* were then manually grouped into *Functional Themes* consisting of related clusters (Table 1). Most apparent in this analysis was the presence of an extracellular matrix (ECM) theme in all three age contrasts, suggesting progressive tissue remodeling with age. There were also strong themes relating to development and transcriptional regulation that became more apparent in the older age contrasts. In particular, there were five clusters associated with regulation of transcription in the contrast between 29 and 24 m. Protein catabolism emerged as a theme in the two oldest age contrasts coincident with the loss of muscle mass in this mouse model (Shavlakadze et al., 2010b). There was also a strong metabolism theme in the comparison of muscles between 29 m and 24 m.

Gene Ontology (GO) enrichments were independently examined using the combined up- and down-regulated genes in each age contrast (Supplementary Table S3). In the age contrast between 24 and 15 m there was confirmation of a strong development theme e.g. *embryonic limb morphogenesis* (Biological Process (BP) GO-0030326, $P = 0.0002$); *regulation of canonical Wnt receptor signalling* (BP GO-0060828, $P = 0.035$); *regulation of smoothened signalling pathway* (BP GO-0008589, $P = 0.006$); *hindlimb morphogenesis* (BP GO-0035137, $P = 0.01$).
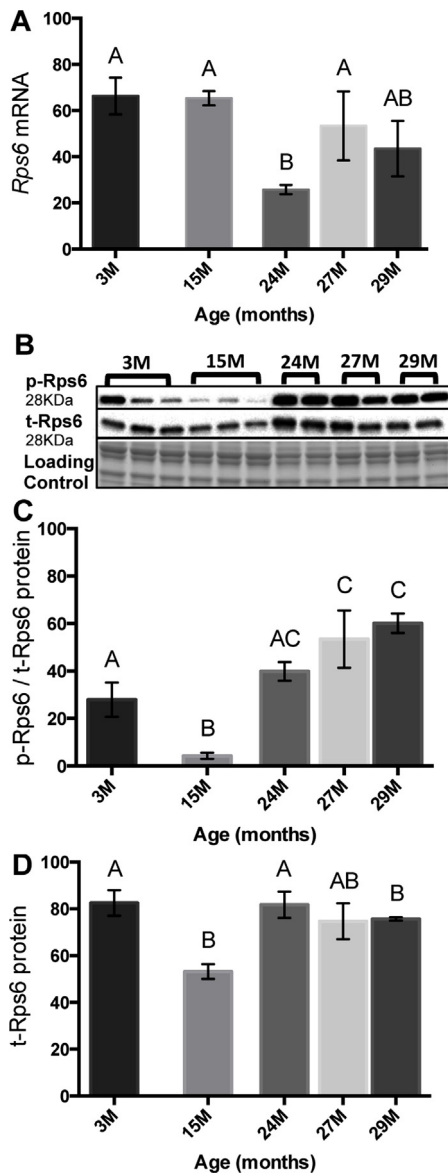
Fig. 5. Rps6 mRNA and protein in quadriceps muscles aged 3–29 m. *Rps6* mRNA (A) was quantified in 4–6 mice/group. For immunoblots, equal loading was confirmed by staining membranes with Ponceau S (B). p-Rps6(Ser235/236) was quantified relative to t-Rps6 (C) and t-Rps6 (D) was quantified relative to a Ponceau S stained band from the same membrane located at ~23 kDa (B). Protein quantification is based on 4 mice/group. Data (A, C and D) are mean ± s.e.m and means without a common letter differ, $P \leq 0.05$, ANOVA with Fisher's LSD tests. Y-axis represents arbitrary units.

An additional enriched GO term in this age contrast (24 and 15 m) included *extracellular region part* (Cellular Component (CC) GO-0044421, $P = 7.6e{-}07$), which contained a number of genes encoding secreted or membrane–bound proteins involved in NMJ function or growth regulatory functions. One gene related to NMJ function was *Prss12* (neurotrypsin; down-regulated 2.7-fold at 24 m) which encodes a synaptic serine protease that cleaves agrin (Stephan et al., 2008). Over-expression of *Prss12* in motoneurons results in disruption of NMJ function and precocious sarcopenia (Butikofer et al., 2011), while humans lacking functional neurotrypsin suffer from severe mental retardation (Molinari et al., 2002; Stephan et al., 2008). Therefore, neurotrypsin dosage is likely to be an important determinant of NMJ function. qRT-PCR analysis of *Prss12* expression in quadriceps (Supplementary Fig. S1D) was consistent with the pronounced decrease at 24 m in gastrocnemius identified in the microarray analysis ($P \leq 0.05$).

Table 1
Summary of the DAVID[a] functional annotation clusters grouped into Functional Themes.

Age contrast months (m)	Up- or down-regulated	Functional Themes[b] (*Functional annotation cluster* number (enrichment score[c]))
15 vs 3 m	Up-regulated	*Apoptosis* (Cluster 1 (2.15)) *Extracellular matrix* (Cluster 2 (1.58); Cluster 4 (1.48)) *Oxido-reductase activity and lipid synthesis* (Cluster 3 (1.51)) *Glucose metabolism* (Cluster 5 (1.3))
15 vs 3 m	Down-regulated	*Extracellular matrix* (Cluster 1 (2.66); Cluster 2 (2.57); Cluster 3 (1.93)) *Development* (Cluster 4 (1.66); Cluster 6 (1.33)).
24 m vs 15 m	Up-regulated	*Regulation of growth and signal transduction* (Cluster 1 (1.57)) *Development* (Cluster 2 (1.5), Cluster 3 (1.3)). *Extracellular matrix* (Cluster 4 (1.27)) *Protein catabolism* (Cluster 5, 1.25))
24 m vs 15 m	Down-regulated	*Apoptosis* (Cluster 1 (1.43))
29 vs 24 m	Up-regulated	*Regulation of transcription* (Cluster 1 (2.68); Cluster 2 (1.73); Cluster 3 (1.64); Cluster 10 (1.14); Cluster 11 (1.12)) *Fatty acid and glucose metabolism* (Cluster 4 (1.61); Cluster 7 (1.27)) *Metabolism* (Cluster 6 (1.49); Cluster 7 (1.27)) *Protein catabolism* (Cluster 5 (1.53); Cluster 12 (1.04)))
29 vs 24 months	Down-regulated	*Regulation of transcription* (Cluster 2 (1.48); *Extracellular matrix* (Cluster 3 (1.32); Cluster 5 (1.05)) *Development* (Cluster 6 (1.04))

[a] Database for Annotation, Visualization and Integrated Discovery (DAVID) (Huang da et al., 2009). The full analysis can be found in Supplementary Table S3.

[b] Functional Themes were defined as a grouping of related *Functional Annotation Clusters*. This higher level process displays similar functional annotations together based on overlaps of genes associated with each function term and therefore gives a clearer overview of gene function information associated with large datasets. The direction of gene expression change is the later age compared with the younger age.

[c] *P*-value LOD scores for enriched terms in each *Functional Annotation Cluster*. Values greater than 1.0 were considered significant.

Ramp1 (receptor activity modifying protein 1; down-regulated 2.5-fold at 24 m) encodes a single-transmembrane protein localized in the NMJ motor endplate where it, in conjunction with the calcitonin-receptor-like receptor (Crlr), form the receptor for calcitonin gene-related peptide. Both Ramp1 and Crlr have putative roles in modulating synaptic transmission at NMJs (Cottrell et al., 2005; Fernandez et al., 2003; Rossi et al., 2003).

Although there were no enrichments for GO terms directly relating to NMJs, there were a number of differentially expressed genes in this age contrast (in addition to those described) that may be relevant (Supplementary File S1). *Emb* (embigin; up-regulated 2.6-fold at 24 m), a transmembrane glycoprotein regulating cell growth and development is located in the NMJ, promotes formation of new motor nerve terminal at NMJs and its transcription is regulated by innervation and promotes NMJ formation and plasticity (Lain et al., 2009). The up-regulation of *Emb* at 24 m may be an indicator of compensatory mechanisms for the decline in NMJ function with age. *Sema5a* (down-regulated by 2.64-fold at 24 m) encodes Semaphorin 5A, a membrane-bound protein involved in axon guidance in non-neural tissues including motor axon outgrowth in myotomes (Hilario et al., 2009). qRT-PCR analysis of expression of *Sema5a* in quadriceps showed no difference between 15 and 24 m although there was a significant decrease between 3 m and all older ages ($P \leq 0.05$) (Supplementary Fig. S1F). Expression of the related gene *Sema3a*, implicated in muscle innervation (Masuda et al., 2013), decreased between 3 and 15 m ($P \leq 0.05$) and
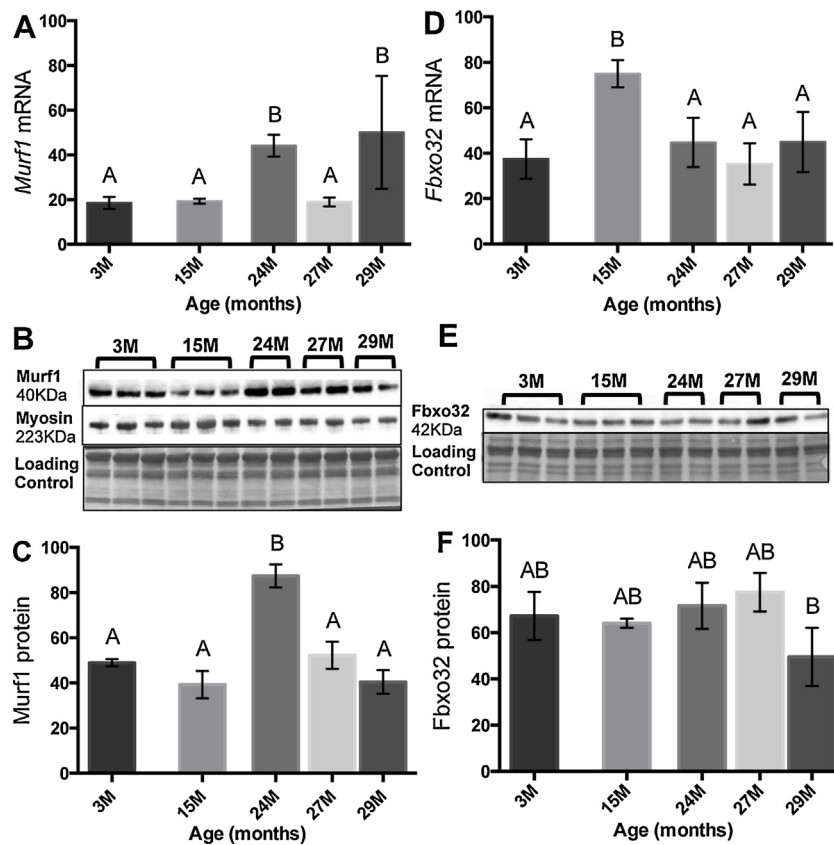
Fig. 6. Murf1 and Fbxo32 (mRNA and protein) in quadriceps muscles aged 3–29 m. *Murf1* (A) and *Fbxo32* (D) mRNA was quantified in 4–6 mice per group. Murf1 protein was detected in 1% NP40 insoluble fraction enriched with myosin heavy chains, which is demonstrated by immunoblotting for the myosin heavy chain (B). The amount of Murf1 protein was quantified (C) relative to a Ponceau S stained band from the same membrane located between 50 and 37 kDa (B) as per (Shavlakadze et al., 2013b). Fbxo32 protein was detected in 1% NP40 soluble fraction and quantified (F) relative to a Ponceau S stained band located at ∼23 kDa (E). Protein quantification is based on 4 mice/group. Data (A, C, D and F) are mean ± s.e.m and means without a common letter differ, $P \leq 0.05$, ANOVA with Fisher's LSD tests. *Y*-axis represents arbitrary units.

progressively increased after 24 m in quadriceps (Supplementary Fig. S1E). *Mdga1* (MAM domain containing glycosylphosphatidylinositol anchor 1; down-regulated 2.2-fold at 24 m) is expressed by multiple tissues including brain, heart and skeletal muscle and it may promote interaction between motoneurons and muscle cells (Fujimura et al., 2006).

Microarray analysis did not identify differential expression of *Chrng* or *Runx1* in gastrocnemius muscle between 15 and 24 m, whereas there were marked differences in mRNA expression as measured by qRT-PCR in quadriceps (Fig. 2A and D). The reason for this disparity may relate to the relatively low level of expression of both genes, which is often associated with increased variance, the differing sensitivities between microarray and qRT-PCR technologies, combined with differences between composition and activities of the two muscles.

Factors involved in angiogenesis were also regulated during the transition from 15 to 24 m. The protein encoded by *Nov* (nephroblastoma over-expressed), a small cysteine-rich secreted protein that binds to the ECM, proposed to act as a stimulator of angiogenesis (Lin et al., 2003) was down-regulated 3.2-fold at 24 m. *Angptl1* (angiopoietin-related-like 1; down-regulated 2.24-fold at 24 m) belongs to the secreted angiopoietin vascular endothelial growth factor family, several of which promote vascularization (Kadomatsu et al., 2011). Thus the combination of decreased *Nov* and *Angptl1* suggests perturbation in angiogenesis.

In addition, the microarray analyses for *Gadd45a* and *Myog* (up-regulated 3.2 and 2.8-fold, respectively at 24 m) were consistent with the qRT-PCR data for quadriceps (Fig. 2E and F). In summary,

the transition from 15 to 24 m may involve changes in NMJ function, angiogenesis and control of myogenesis.

Muscle mass relative to body size diminished significantly between the ages of 24 and 29 m signifying the progression of 'pathology' associated with sarcopenia (Brayton et al., 2012; Sundberg et al., 2011). Correspondingly, there is an increased number of differentially expressed genes in this age contrast compared to the earlier age contrasts (Supplementary Table S2) and enrichment for GO terms relating to regulation of gene transcription (Molecular Function (MF) GO-0003700, $P = 0.003$; MF GO-0043565, $P = 0.005$) (Supplementary File S1), which collectively suggest perturbation of transcriptional control. The enriched KEGG pathway, *biosynthesis of unsaturated fatty acids* (KEGG-01040; $P = 0.001$) for this age contrast primarily reflected up-regulation of three acyl-CoA-thioesterases (respectively 9.0, 7.36 and 3.92-fold up-regulation at 29 m), up-regulation of uncoupling protein 3 (*Ucp3*; 2.1-fold) and down-regulation of stearoyl-coenzyme A desaturase I (*Scd1*; 9.78-fold) and suggest altered mitochondrial fatty acid metabolism. The up-regulation of several genes involved in fatty acid biosynthesis at 29 m may signify greater demand for fatty acid oxidation, perhaps associated with age-related decline in overall mitochondrial function (Short et al., 2005).

3.5. The effect of ageing on global gene expression variance

The age-related increase in the number of differentially expressed genes and differential expression of homeobox containing transcription factors at 29 m compared with 24 m
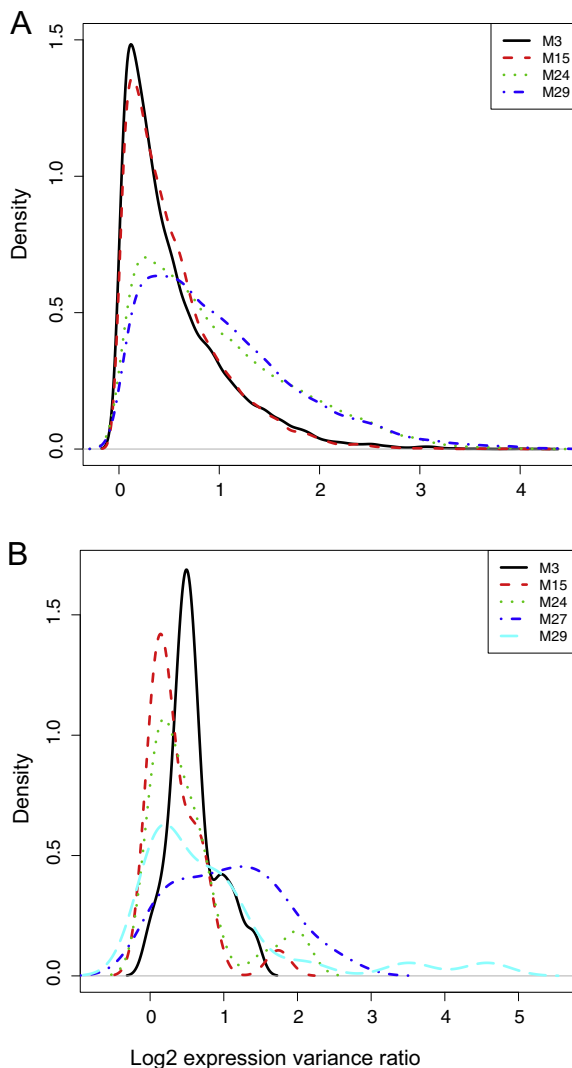
A

B

Fig. 7. Density plot of gene expression data variance ratios (within group variance divided by total variance) for each age group. (A) Gene expression variance devised from microarray data. (B) Gene expression variance devised from qRT-PCR expression data. Aged groups (24, 27 and 29 m) show higher variation in gene expression intensities compared with the younger groups (3 and 15 m).

(Supplementary File S1 and Table S3) suggested changes in global gene expression regulation with age. To investigate this aspect, the gene expression variance associated with the microarray and qRT-PCR data for gastrocnemius and quadriceps muscles, respectively, was analyzed. A density plot of variance ratios for each age group from the microarray data (Fig. 7A) demonstrates that the 24 and 29 m gene expression data have much higher overall variance compared with profiles for younger ages. The variance ratios for each age were all significantly different from each other ($P = 0$, except for ages 24 m paired with 29 m where $P = 0.002$). Age 15 m shows the lowest variance and, in relation to this age group, the variance ratios for other ages are 1.15 (3 m), 2.35 (24 m) and 2.47 (29 m). Similar results were also apparent from analysis of variance for the qRT-PCR data for 23 genes (Fig. 7B). In contrast to the array data, age 3 m exhibited lower overall variance in relation to 15 m with a ratio of 0.72. Ages 24 and 27 m had, respectively, variance ratios of 2.19 and 3.31 compared with 15 m. The oldest age group (29 m) had an even higher ratio of 8.49. Collectively, these data indicate that global gene expression variance increases in old mice and becomes progressively more pronounced with senescence.

4. Discussion

The time course analysis across five ages (3–29 m) in mice has significantly advanced our understanding of the interacting molecular mechanisms that are associated with the onset and progression of sarcopenia. A central theme is myofibre denervation that is pronounced by 24 m (not evident at 15 m), and also inferred from age-related changes in the protein metabolism pathways. These comprehensive results, combined with microarray global analyses are discussed below.

4.1. Molecular markers of myofibre denervation in ageing muscles

Transcriptional analyses by qRT-PCR of quadriceps muscles and microarray of gastrocnemius muscles from female mice aged 3–29 m support the proposal that disturbances in muscle innervation, including loss of NMJs are pronounced by the time loss of muscle mass (sarcopenia) is evident at 24 m. Increased expression of nAChR subunits γ and δ, *Ncam1* and *Myog* at 24 m, in marked contrast with the low levels in fully mature 15 m old muscles, points to disturbances in NMJs, because these genes are normally suppressed by innervation (Adams et al., 1995; Dedkov et al., 2003; Hall and Sanes, 1993; Kostrominova et al., 2000; Wang et al., 2005; Zhu et al., 1994). The strong induction of *Runx1* in old mouse muscles, also observed in old rat muscles (Ibebunjo et al., 2013), may also indicate the presence of denervated myofibres: Runx1 expression increases in surgically denervated muscle (Zhu et al., 1994) and is proposed to protect myofibres from severe atrophy (Wang et al., 2005). Up-regulation of *Gadd45a* from 15 to 24 m detected by qRT-PCR and microarray also points to muscle denervation. In fact, a recent study indicates that Gadd45a mediates denervation-induced myofibre atrophy (the mechanism is not fully understood) and forced expression of *Gadd45a* increases expression of the embryonic nAChR γ subunit (Bongers et al., 2013).

In ageing muscle it can be difficult to identify the precise reason for increased expression of genes regulated by innervation since degeneration of NMJs, as well as muscle regeneration, can result in re-expression of such genes, normally suppressed by innervation (Eftimie et al., 1991; Moresi et al., 2010). In our study in old female C57Bl/6J quadriceps, there was no histological indication that necrosis or regeneration was occurring, and myofibres with non-peripheral nuclei were not conspicuous before 29 m. It should be noted that although non-peripheral (central) myonuclei are used as a marker to identify regenerated myofibres in mature postnatal muscle (McGeachie et al., 1993), internalization of myonuclei also becomes increasingly common in long-term denervated muscles (Lu et al., 1997).

Microarray analyses of ageing gastrocnemius reinforced the view (from targeted qRT-PCR analyses for quadriceps muscle) that the period between 15 and 24 m, when loss of muscle mass first became evident (Shavlakadze et al., 2010b), is associated with disruption of transcription of genes involved in NMJ function. These genes encode proteins that impact NMJ function (Prss12 and Ramp1) (Butikofer et al., 2011; Cottrell et al., 2005; Fernandez et al., 2003; Molinari et al., 2002; Rossi et al., 2003; Stephan et al., 2008) and factors that promote formation of new NMJs (Embigin and Mdga1) (Fujimura et al., 2006; Lain et al., 2009).

4.2. Protein synthesis and degradation pathways

This study demonstrates that decreased muscle mass in old C57Bl/6J female mice occurs in conjunction with increased Igf1r and Rps6 protein amounts and increased Rps6 phosphorylation; with no changes in Akt phosphorylation. Reduced Igf1r has been proposed as one reason for sarcopenia (Urso et al., 2005) and

two studies report reduced Igf1r protein levels in limb muscles of 24–25 m old female C57Bl/6J mice compared with young mice (Li et al., 2003; Martineau et al., 1999). Both studies used mice that were food deprived for 12 h or more (Li et al., 2003; Martineau et al., 1999), which may account for the discrepancy with our study where Igf1r protein was increased in quadriceps muscles of freely fed female C57Bl/6J mice aged 24 m and older, compared with 15 m. Our observation is in agreement with increased Igf1r in gastrocnemius muscles of freely fed male and female rats aged 30 m, compared with 6 and 12 m, respectively (Edstrom et al., 2006; Haddad and Adams, 2006). It is possible that accumulation of Igf1r protein in old muscles is due to reduced degradation of this protein. We did not measure phosphorylation of Igf1r; however other studies report no difference in Igf1r phosphorylation in 30 m old rat muscles compared with 6 m (Haddad and Adams, 2006) and, in mice, intraperitoneal administration of IGF-1 stimulated basal levels of skeletal muscle Akt phosphorylation with equal efficacy at 5 and 24 m (Li et al., 2003). Thus, at least in rodents, old skeletal muscle may not be deficient in Igf1r protein amount, although the rates of Igf1r turnover in old muscles require further investigation.

To evaluate signalling downstream from Igf1r, we measured total and phosphorylated Akt and Rps6 proteins in quadriceps muscles at all ages (3–29 m). Akt is the key protein that mediates signalling downstream from the activated receptors for Igf1 and insulin. Akt promotes protein synthesis by activating the mammalian target of rapamycin complex 1 (mTORC1) and may impede protein degradation by suppressing expression of E3 ubiquitin-protein ligases (reviewed in Glass, 2003; Schiaffino and Mammucari, 2011). Rps6 is a downstream target for S6K1 and becomes phosphorylated with activation of the mTORC1 pathway (Ruvinsky and Meyuhas, 2006). The lower protein levels of total Akt and total and phosphorylated Rps6 at 15 m compared with 3 m are likely to be due to muscle maturation, since muscle mass continues to increase after 3 m (Shavlakadze et al., 2010b). Decreased activity of signalling molecules downstream of the Igf1/insulin receptors has also been shown in maturing muscles of pigs (Davis and Fiorotto, 2009; Suryawan et al., 2007).

Increased total Akt and Rps6 protein and phosphorylated Rps6(S235/236) in old quadriceps accord with other reports for old rodent muscles (Haddad and Adams, 2006; Sandri et al., 2013), although the precise reasons for these increases in ageing atrophic muscle are not known. Disturbances in NMJs (myofibre denervation) in old muscle may be a contributing factor (Machida et al., 2012; Norrby et al., 2012), since Akt and RpS6 protein amounts and their phosphorylation are increased in murine muscle surgically denervated for up to 2 weeks (Machida et al., 2012; Norrby et al., 2012). Whether the increased Rps6 phosphorylation in old murine muscles seen in our and another recent study (Sandri et al., 2013) translates into increased protein synthesis in not known. However in ageing Sprague-Dawley rats progressive muscle loss occurs in conjunction with elevated protein synthesis (Kimball et al., 2004).

An important aspect of our research is the demonstration of a time-course for Murf1 and Fbxo32 expression during muscle maturation and ageing. Murf1 is a muscle-specific ubiquitin ligase that facilitates degradation of thick filaments during muscle atrophy (Clarke et al., 2007; Cohen et al., 2009). The biological role of Fbxo32 is less well understood, however it is proposed that Fbxo32 controls protein synthesis by degrading eIF3f and thus suppressing S6K1 activation by mTORC1 (Csibi et al., 2010).

Reports on the regulation of Murf1 and Fbxo32 in ageing muscle are inconsistent, probably due to sampling of limited ages (usually one old group) (Clavel et al., 2006; Edstrom et al., 2006; Gaugler et al., 2011). In addition, most studies measure transcript but not protein levels (Demontis et al., 2013). In our study, up-regulation of Murf1 mRNA and protein at 24 m coincided with increased expression of muscle denervation markers; indicating that Murf1 may be transiently up-regulated during earlier stages of myofibre denervation. Decreased *Fbxo32* mRNA and protein has been previously reported in ageing rat muscles (Edstrom et al., 2006), although the implications of decreased Fbxo32 in ageing muscle are unclear.

Increased *Murf1* mRNA in 24 m quadriceps occurred without a change in Akt phosphorylation, which is a major suppressor of *Murf1* expression (Sacheck et al., 2004; Stitt et al., 2004). Similar disconnection between Akt phosphorylation and *Murf1* and *Fbxo32* expression occurs in surgically denervated muscle (Machida et al., 2012; Norrby et al., 2012), where *Murf1* and *Fbxo32* mRNA increases (Moresi et al., 2010) in conjunction with elevated Akt phosphorylation (Machida et al., 2012; Norrby et al., 2012). Myogenin has been proposed to drive Murf1 and Fbxo32 expression in surgically denervated muscles (Moresi et al., 2010). In our study, *Myogenin* mRNA increased at 24, 27 and 29 m. If myogenin is responsible for age-related up-regulation of Murf1 at 24 m, it is not clear why high levels of Murf1 are not maintained at older ages. Thus, further studies are required to identify regulators of Murf1 expression in the old muscle.

The microarray analyses helped validate the functional themes investigated using the targeted approaches and revealed additional themes associated with the emergence of sarcopenia in mice. The microarray analyses of ageing gastrocnemius muscle indicated that the Functional Theme *Protein catabolism* was first discernable in the 15 and 24 age contrast and then again in the age contrast between 24 m and 29 m. These results are consistent with data showing that the former period is associated with the transition to loss of muscle mass (Shavlakadze et al., 2010b).

A common Functional Theme in all age contrasts from the microarray analysis was *extracellular matrix* (ECM) suggesting continual remodeling of skeletal muscle during ageing. The effects of ECM on all aspects of skeletal muscle formation and function are highly complex (Grounds, 2008) and intrinsic muscle cell function is likely to alter as a consequence of these age-related ECM changes. Metabolic traits, particularly those involving altered fatty acid metabolism, were apparent in the contrast between 24 m and 29 m. This may reflect inefficiency of lipid metabolism with ageing caused by altered mitochondrial function, which has been implicated in ageing processes in other studies (Demontis et al., 2013). In the present study we did not measure the activity levels of the ageing mice. General age-associated decline in physical activity in mice (McMahon et al., 2014) may contribute to the decline in mitochondrial function in addition to the ageing process *per se*.

There were no functional themes associated with oxidative stress, inflammation nor immune cell infiltration in any age contrast, indicating that these factors may not be primary drivers of sarcopenia. Other studies in mice also did not identify up-regulation of genes linked to inflammatory response in old skeletal muscles (Weindruch et al., 2001).

The striking increase of gene expression variance with age indicates a systematic age-related decrease in regulation of transcription. Other studies have noted a similar effect in ageing rat retina (Li et al., 2009), human brain, kidney, skeletal muscle (Somel et al., 2006), *C. elegans* (Vinuela et al., 2010) and mouse heart (Bahar et al., 2006). It is noteworthy for the differentially expressed genes between 24 and 29 m that there was enrichment for the functional theme *regulation of transcription* in both the up- and down-regulated genes, which could serve to amplify any general increase in gene expression variance. The enrichment of the Functional Theme *development*, particularly for genes up-regulated between 15 and 24 m, involves a number of homeobox encoding transcription factors and pioneering transcription factors: these genes are typically active in early development, however our results indicate that they also have roles in mature muscle tissues. It is possible that these core developmental transcription factor changes are priming altered expression of other transcription factors at the

later ages, which in turn may contribute to the enhanced gene expression variance with age. One possibility is that epigenetic controls on gene transcription, particularly developmental transcription factors, are becoming less robust with age.

Overall, the molecular changes in the ageing female C57Bl/6J muscles strongly reinforce the central role for myofibre denervation that may also explain changes in expression of proteins involved in regulating protein synthesis and degradation, the imbalance of which is the primary outcome of sarcopenia. The key findings were (1) strong molecular confirmation of myofibre denervation during the transition to sarcopenia (15–24 m) with some of these mRNA changes (e.g. *Chrng, Runx1, Gadd45α, Myogenin*) representing potentially useful biomarkers; (2) decreased muscle mass occurring in conjunction with increased mTORC1 signalling (Rps6 phosphorylation); (3) transient elevation of Murf1, associated with myofibrillar protein degradation; (4) no evidence for a role of inflammation in sarcopenia development nor pathology; (5) a role for ECM remodelling; (6) potential role of mitochondria dysfunction in the pathology but not the initiation of sarcopenia, and; (7) enhanced global gene expression variance with ageing.

Acknowledgments

Appendix A. Supplementary data

Supplementary data associated with this article can be found, in the online version, at http://dx.doi.org/10.1016/j.biocel.2014.04.025.

References

Aagaard P, Suetta C, Caserotti P, Magnusson SP, Kjaer M. Role of the nervous system in sarcopenia and muscle atrophy with aging: strength training as a countermeasure. Scand J Med Sci Sports 2010;20:49–64.

Adams L, Carlson BM, Henderson L, Goldman D. Adaptation of nicotinic acetylcholine receptor, myogenin, and MRF4 gene expression to long-term muscle denervation. J Cell Biol 1995;131:1341–9.

Alexa A, Rahnenfuhrer J. Gene set enrichment analysis with topGO; 2013, www.bioconductor.org

Altun M, Besche HC, Overkleeft HS, Piccirillo R, Edelmann MJ, Kessler BM, et al. Muscle wasting in aged, sarcopenic rats is associated with enhanced activity of the ubiquitin proteasome pathway. J Biol Chem 2010;285:39597–608.

Bahar R, Hartmann CH, Rodriguez KA, Denny AD, Busuttil RA, Dolle ME, et al. Increased cell-to-cell variation in gene expression in ageing mouse heart. Nature 2006;441:1011–4.

Bongers KS, Fox DK, Ebert SM, Kunkel SD, Dyle MC, Bullard SA, et al. Skeletal muscle denervation causes skeletal muscle atrophy through a pathway that involves both Gadd45a and HDAC4. Am J Physiol Endocrinol Metab 2013;305:E907–15.

Brayton CF, Treuting PM, Ward JM. Pathobiology of aging mice and GEM: background strains and experimental design. Vet Pathol 2012;49:85–105.

Butikofer L, Zurlinden A, Bolliger MF, Kunz B, Sonderegger P. Destabilization of the neuromuscular junction by proteolytic cleavage of agrin results in precocious sarcopenia. FASEB J 2011;25:4378–93.

Calvani R, Joseph AM, Adhihetty PJ, Miccheli A, Bossola M, Leeuwenburgh C, et al. Mitochondrial pathways in sarcopenia of aging and disuse muscle atrophy. Biol Chem 2013;394:393–414.

Chai RJ, Vukovic J, Dunlop S, Grounds MD, Shavlakadze T. Striking denervation of neuromuscular junctions without lumbar motoneuron loss in geriatric mouse muscle. PLoS One 2011;6:e28090.

Clark BC, Manini TM. Sarcopenia =/= dynapenia. J Gerontol A Biol Sci Med Sci 2008;63:829–34.

Clarke BA, Drujan D, Willis MS, Murphy LO, Corpina RA, Burova E, et al. The E3 Ligase MuRF1 degrades myosin heavy chain protein in dexamethasone-treated skeletal muscle. Cell Metab 2007;6:376–85.

Clavel S, Coldefy AS, Kurkdjian E, Salles J, Margaritis I, Derijard B. Atrophy-related ubiquitin ligases, atrogin-1 and MuRF1 are up-regulated in aged rat Tibialis Anterior muscle. Mech Ageing Dev 2006;127:794–801.

Cohen S, Brault JJ, Gygi SP, Glass DJ, Valenzuela DM, Gartner C, et al. During muscle atrophy, thick, but not thin, filament components are degraded by MuRF1-dependent ubiquitylation. J Cell Biol 2009;185:1083–95.

Cottrell GS, Roosterman D, Marvizon JC, Song B, Wick E, Pikios S, et al. Localization of calcitonin receptor-like receptor and receptor activity modifying protein 1 in enteric neurons, dorsal root ganglia, and the spinal cord of the rat. J Comp Neurol 2005;490:239–55.

Cruz-Jentoft AJ. Sarcopenia: European consensus on definition and diagnosis. Age Ageing 2010;39:412–23.

Csibi A, Cornille K, Leibovitch MP, Poupon A, Tintignac LA, Sanchez AM, et al. The translation regulatory subunit eIF3f controls the kinase-dependent mTOR signaling required for muscle differentiation and hypertrophy in mouse. PLoS ONE 2010;5:e8994.

Davis TA, Fiorotto ML. Regulation of muscle growth in neonates. Curr Opin Clin Nutr Metab Care 2009;12:78–85.

Dedkov EI, Kostrominova TY, Borisov AB, Carlson BM. MyoD and myogenin protein expression in skeletal muscles of senile rats. Cell Tissue Res 2003;311:401–16.

Demontis F, Piccirillo R, Goldberg AL, Perrimon N. Mechanisms of skeletal muscle aging: insights from Drosophila and mammalian models. Dis Models Mech 2013;6:1339–52.

Edstrom E, Altun M, Hagglund M, Ulfhake B. Atrogin-1/MAFbx and MuRF1 are down-regulated in aging-related loss of skeletal muscle. J Gerontol A Biol Sci Med Sci 2006;61:663–74.

Eftimie R, Brenner HR, Buonanno A. Myogenin and MyoD join a family of skeletal muscle genes regulated by electrical activity. Proc Natl Acad Sci USA 1991;88:1349–53.

Faulkner JA, Larkin LM, Claflin DR, Brooks SV. Age-related changes in the structure and function of skeletal muscles. Clin Exp Pharmacol Physiol 2007;34:1091–6.

Fernandez HL, Chen M, Nadelhaft I, Durr JA. Calcitonin gene-related peptides: their binding sites and receptor accessory proteins in adult mammalian skeletal muscles. Neuroscience 2003;119:335–45.

Flurkey K, Currer JM, Harrison DE. The mouse in aging research. Burlington, MA: American College Laboratory Animal Medicine (Elsevier); 2007.

Fujimura Y, Iwashita M, Matsuzaki F, Yamamoto T. MDGA1, an IgSF molecule containing a MAM domain, heterophilically associates with axon- and muscle-associated binding partners through distinct structural domains. Brain Res 2006;1101:12–9.

Gaugler M, Brown A, Merrell E, DiSanto-Rose M, Rathmacher JA, Reynolds T. Ht. PKB signaling and atrogene expression in skeletal muscle of aged mice. J Appl Physiol 2011;111:192–9.

Gentleman RC, Carey VJ, Bates DM, Bolstad B, Dettling M, Dudoit S, et al. Bioconductor: open software development for computational biology and bioinformatics. Genome Biol 2004;5:R80.

Glass DJ. Signalling pathways that mediate skeletal muscle hypertrophy and atrophy. Nat Cell Biol 2003;5:87–90.

Grounds MD. Complexity of extracellular matrix and skeletal muscle regeneration. In: Schiaffino S, Partridge TA, editors. Skeletal muscle repair and regeneration. Netherlands: Springer; 2008. p. 269–302 [chapter 13].

Haddad F, Adams GR. Aging-sensitive cellular and molecular mechanisms associated with skeletal muscle hypertrophy. J Appl Physiol 2006;100:1188–203.

Hall ZW, Sanes JR. Synaptic structure and development: the neuromuscular junction. Cell 1993;72(Suppl.):99–121.

Hilario JD, Rodino-Klapac LR, Wang C, Beattie CE. Semaphorin 5A is a bifunctional axon guidance cue for axial motoneurons in vivo. Dev Biol 2009;326: 190–200.

Huang da W, Sherman BT, Lempicki RA. Systematic and integrative analysis of large gene lists using DAVID bioinformatics resources. Nat Protoc 2009;4:44–57.

Ibebunjo C, Chick JM, Kendall T, Eash JK, Li C, Zhang Y, et al. Genomic and proteomic profiling reveals reduced mitochondrial function and disruption of the neuromuscular junction driving rat sarcopenia. Mol Cell Biol 2013;33:194–212.

Irizarry RA, Bolstad BM, Collin F, Cope LM, Hobbs B, Speed TP. Summaries of Affymetrix GeneChip probe level data. Nucleic Acids Res 2003a;31:e15.

Irizarry RA, Hobbs B, Collin F, Beazer-Barclay YD, Antonellis KJ, Scherf U, et al. Exploration, normalization, and summaries of high density oligonucleotide array probe level data. Biostatistics 2003b;4:249–64.

Janssen I. Evolution of sarcopenia research. Appl Physiol Nutr Metab 2010;35:707–12.

Kadomatsu T, Tabata M, Oike Y. Angiopoietin-like proteins: emerging targets for treatment of obesity and related metabolic diseases. FEBS J 2011;278:559–64.

Kimball SR, O'Malley JP, Anthony JC, Crozier SJ, Jefferson LS. Assessment of biomarkers of protein anabolism in skeletal muscle during the life span of the rat: sarcopenia despite elevated protein synthesis. Am J Physiol Endocrinol Metab 2004;287:E772–80.

Kostrominova TY, Macpherson PCD, Carlson BM, Goldman D. Regulation of myogenin protein expression in denervated muscles from young and old rats. Am J Physiol Regul Integr Comp Physiol 2000;279:R179–88.

Lain E, Carnejac S, Escher P, Wilson MC, Lomo T, Gajendran N, et al. A novel role for embigin to promote sprouting of motor nerve terminals at the neuromuscular junction. J Biol Chem 2009;284:8930–9.

Li M, Li C, Parkhouse WS. Age-related differences in the des IGF-I-mediated activation of Akt-1 and p70 S6K in mouse skeletal muscle. Mech Ageing Dev 2003;124:771–8.

Li Z, Wright FA, Royland J. Age-dependent variability in gene expression in male Fischer 344 rat retina. Toxicol Sci 2009;107:281–92.

Lin CG, Leu SJ, Chen N, Tebeau CM, Lin SX, Yeung CY, et al. CCN3 (NOV) is a novel angiogenic regulator of the CCN protein family. J Biol Chem 2003;278:24200–8.

Lu D-X, Huang S-K, Carlson BM. Electron microscopic study of long-term denervated rat skeletal muscle. Anat Rec 1997;248:355–65.

Machida M, Takeda K, Yokono H, Ikemune S, Taniguchi Y, Kiyosawa H, et al. Reduction of ribosome biogenesis with activation of the mTOR pathway in denervated atrophic muscle. J Cell Physiol 2012;227:1569–76.

Martineau LC, Chadan SG, Parkhouse WS. Age-associated alterations in cardiac and skeletal muscle glucose transporters, insulin and IGF-1 receptors, and PI3-kinase protein contents in the C57BL/6 mouse. Mech Ageing Dev 1999;106:217–32.

Masuda T, Taniguchi M, Sakuma C, Yamagishi T, Ueda S, Kawaguchi M, et al. Development of the dorsal ramus of the spinal nerve in the mouse embryo: involvement of semaphorin 3A in dorsal muscle innervation. Congenit Anom 2013;53:122–6.

McGeachie JK, Grounds MD, Partridge TA, Morgan JE. Age-related changes in replication of myogenic cells in mdx mice: quantitative autoradiographic studies. J Neurol Sci 1993;119:169–79.

McMahon C, Shavlakadze T, Grounds M. Role of IGF-I in age-related loss of skeletal muscle mass and function. In: Lynch GS, editor. Sarcopenia – age-related muscle wasting and weakness. Netherlands: Springer; 2010. p. 395–418.

McMahon C, Chai R, Radley-Crabb HG, Watson T, Matthews KG, Sheard PW, et al. Lifelong exercise and locally produced insulin-like growth factor-1 (IGF-1) have a modest influence on reducing age-related muscle wasting in mice. Scand J Med Sci Sports 2014., http://dx.doi.org/10.1111/sms.12200.

Molinari F, Rio M, Meskenaite V, Encha-Razavi F, Auge J, Bacq D, et al. Truncating neurotrypsin mutation in autosomal recessive nonsyndromic mental retardation. Science 2002;298:1779–81.

Moresi V, Williams AH, Meadows E, Flynn JM, Potthoff MJ, McAnally J, et al. Myogenin and class II HDACs control neurogenic muscle atrophy by inducing E3 ubiquitin ligases. Cell 2010;143:35–45.

Nader GA. Molecular determinants of skeletal muscle mass: getting the "AKT" together. Int J Biochem Cell Biol 2005;37:1985–96.

Norrby M, Evertsson K, Fjallstrom AK, Svensson A, Tagerud S. Akt (protein kinase B) isoform phosphorylation and signaling downstream of mTOR (mammalian target of rapamycin) in denervated atrophic and hypertrophic mouse skeletal muscle. J Mol Signal 2012;7:7.

Rennie MJ, Selby A, Atherton P, Smith K, Kumar V, Glover EL, et al. Facts, noise and wishful thinking: muscle protein turnover in aging and human disuse atrophy. Scand J Med Sci Sports 2010;20:5–9.

Rossi SG, Dickerson IM, Rotundo RL. Localization of the calcitonin gene-related peptide receptor complex at the vertebrate neuromuscular junction and its role in regulating acetylcholinesterase expression. J Biol Chem 2003;278:24994–5000.

Ruvinsky I, Meyuhas O. Ribosomal protein S6 phosphorylation: from protein synthesis to cell size. Trends Biochem Sci 2006;31:342–8.

Sacheck JM, Ohtsuka A, McLary SC, Goldberg AL. IGF-I stimulates muscle growth by suppressing protein breakdown and expression of atrophy-related ubiquitin ligases, atrogin-1 and MuRF1. Am J Physiol Endocrinol Metab 2004;287:E591–601.

Sandri M, Barberi L, Bijlsma AY, Blaauw B, Dyar KA, Milan G, et al. Signalling pathways regulating muscle mass in ageing skeletal muscle. The role of the IGF1-Akt-mTOR-FoxO pathway. Biogerontology 2013;14:303–23.

Sayer AA, Robinson SM, Patel HP, Shavlakadze T, Cooper C, Grounds MD. New horizons in the pathogenesis, diagnosis and management of sarcopenia. Age Ageing 2013;42:145–50.

Schiaffino S, Mammucari C. Regulation of skeletal muscle growth by the IGF1-Akt/PKB pathway: insights from genetic models. Skeletal Muscle 2011;1:4.

Shavlakadze T, Anwari T, Soffe Z, Cozens G, Mark PJ, Gondro C, et al. Impact of fasting on the rhythmic expression of myogenic and metabolic factors in skeletal muscle of adult mice. Am J Physiol Cell Physiol 2013a;305:C26–35.

Shavlakadze T, Chai J, Maley K, Cozens G, Grounds G, Winn N, et al. A growth stimulus is needed for IGF-1 to induce skeletal muscle hypertrophy in vivo. J Cell Sci 2010a;123:960–71.

Shavlakadze T, Grounds M. Of bears, frogs, meat, mice and men: complexity of factors affecting skeletal muscle mass and fat. BioEssays 2006;28:994–1009.

Shavlakadze T, Grounds MD. Therapeutic interventions for age-related muscle wasting: importance of innervation and exercise for preventing sarcopenia. In: Rattan S, editor. Modulating aging and longevity. Great Britain: Kluwer Academic Publishers; 2003. p. 139–66.

Shavlakadze T, McGeachie J, Grounds MD. Delayed but excellent myogenic stem cell response of regenerating geriatric skeletal muscles in mice. Biogerontology 2010b;11:363–76.

Shavlakadze T, Soffe Z, Anwari T, Cozens G, Grounds MD. Short-term feed deprivation rapidly induces the protein degradation pathway in skeletal muscles of young mice. J Nutr 2013b;143:403–9.

Short KR, Bigelow ML, Kahl J, Singh R, Coenen-Schimke J, Raghavakaimal S, et al. Decline in skeletal muscle mitochondrial function with aging in humans. Proc Natl Acad Sci USA 2005;102:5618–23.

Smyth GK. Linear models and empirical bayes methods for assessing differential expression in microarray experiments. Stat Appl Genet Mol Biol 2004;3:Article3.

Somel M, Khaitovich P, Bahn S, Paabo S, Lachmann M. Gene expression becomes heterogeneous with age. Curr Biol 2006;16:R359–60.

Stephan A, Mateos JM, Kozlov SV, Cinelli P, Kistler AD, Hettwer S, et al. Neurotrypsin cleaves agrin locally at the synapse. FASEB J 2008;22:1861–73.

Stitt TN, Drujan D, Clarke BA, Panaro F, Timofeyva Y, Kline WO, et al. The IGF-1/PI3K/Akt pathway prevents expression of muscle atrophy-induced ubiquitin ligases by inhibiting FOXO transcription factors. Mol Cell 2004;14:395–403.

Sundberg JP, Berndt A, Sundberg BA, Silva KA, Kennedy V, Bronson R, et al. The mouse as a model for understanding chronic diseases of aging: the histopathologic basis of aging in inbred mice. Pathobiol Aging Age Relat Dis 2011;1., http://dx.doi.org/10.3402/pba.v1i0.7179, Epub 2011 Jun 1.

Suryawan A, Orellana RA, Nguyen HV, Jeyapalan AS, Fleming JR, Davis TA. Activation by insulin and amino acids of signaling components leading to translation initiation in skeletal muscle of neonatal pigs is developmentally regulated. Am J Physiol Endocrinol Metab 2007;293:E1597–605.

Tohma H, Hepworth AR, Shavlakadze T, Grounds MD, Arthur PG. Quantification of ceroid and lipofuscin in skeletal muscle. J Histochem Cytochem 2011;59:769–79.

Urso ML, Fiatarone Singh MA, Ding W, Evans WJ, Cosmas AC, Manfredi TG. Exercise training effects on skeletal muscle plasticity and IGF-1 receptors in frail elders. Age (Dordr) 2005;27:117–25.

Valdez G, Tapia JC, Kang H, Clemenson GD Jr, Gage FH, Lichtman JW, et al. Attenuation of age-related changes in mouse neuromuscular synapses by caloric restriction and exercise. Proc Natl Acad Sci USA 2010;107:14863–8.

Vandesompele J, De Preter K, Pattyn F, Poppe B, Van Roy N, De Paepe A, et al. Accurate normalization of real-time quantitative RT-PCR data by geometric averaging of multiple internal control genes. Genome Biol 2002;3, RESEARCH0034.

Vinuela A, Snoek LB, Riksen JA, Kammenga JE. Genome-wide gene expression regulation as a function of genotype and age in *C. elegans*. Genome Res 2010;20:929–37.

Wang X, Blagden C, Fan J, Nowak SJ, Taniuchi I, Littman DR, et al. Runx1 prevents wasting, myofibrillar disorganization, and autophagy of skeletal muscle. Genes Dev 2005;19:1715–22.

Weindruch R, Kayo T, Lee CK, Prolla TA. Microarray profiling of gene expression in aging and its alteration by caloric restriction in mice. J Nutr 2001;131:918S–23S.

Yang F, Wang W, Li J, Haines S, Asher G, Li C. Antler development was inhibited or stimulated by cryosurgery to periosteum or skin in a central antlerogenic region respectively. J Exp Zool B Mol Dev Evol 2011;316:359–70.

Zhu X, Yeadon JE, Burden SJ. AML1 is expressed in skeletal muscle and is regulated by innervation. Mol Cell Biol 1994;14:8051–7.